ROLE OF GRAIN BOUNDARY CARBIDES IN CRACKING BEHAVIOR OF Ni BASE ALLOYS

SEONG SIK HWANG[*], YUN SOO LIM, SUNG WOO KIM, DONG JIN KIM, and HONG PYO KIM
Nuclear Materials Research Division, Korea Atomic Energy Research Institute
989-111 Daedeog-daero, Yuseong-gu, Daejeon, 305-353, Republic of Korea
[*]Corresponding author. E-mail : sshwang@kaeri.re.kr

The primary water stress corrosion cracking (PWSCC) of Alloy 600 in a PWR has been reported in the control rod drive mechanism (CRDM), pressurizer instrumentation, and the pressurizer heater sleeves. Recently, two cases of boric acid precipitation that indicated leaking of the primary cooling water were reported on the bottom head surface of steam generators (SG) in Korea. The PWSCC resistance of Ni base alloys which have intergranular carbides is higher than those which have intragranular carbides. Conversely, in oxidized acidic solutions like sodium sulfate or sodium tetrathionate solutions, the Ni base alloys with a lot of carbides at the grain boundaries and shows less stress corrosion cracking (SCC) resistance. The role of grain boundary carbides in SCC behavior of Ni base alloys was evaluated and effect of intergranular carbides on the SCC susceptibility were reviewed from the literature.

1. INTRODUCTION

The primary water stress corrosion cracking (PWSCC) of Alloy 600 in a pressurized water reactor (PWR) has been reported in the control rod drive mechanism (CRDM), pressurizer instrumentation, and the pressurizer heater[1-4]. In the original PWRs, PWSCC was not appropriately considered. Beginning in the mid-seventies, the PWR plants suffered from a sequence of PWSCC events which were mostly confined to S/G tubes, initially ODSCC then PWSCC. In forged Alloy 600 materials, PWSCC was first reported in the Bugey 3 vessel head penetration in September 1991. All reactor vessel heads (RVH) with Alloy 600 penetrations (54 RVH out of 58) were replaced in France. Other PWRs experienced cracking, which was attributed to the PWSCC of the major primary side welds made from Alloy 182 at the end of the year 2000. The three events concerned had dissimilar metal butt welds between the main austenitic stainless steel primary circuit piping and the outlet pressure vessel nozzles of Ringhals 4 and V. C. Summer and some J-groove welds of the CRDM of the RVH at Oconee 1 [4].

In addition to the RVH, PWSCC of Alloy 182/82 has been reported at bottom mounted instrumentation (BMI) nozzle J-welds, steam generator (SG) drain J-welds, drain nozzles and SG tube sheet cladding. Since 2006, 344 PWSCC incidents of Alloy 600/82/182 were reported in RVH, SG, Pressurizer, and other primary side piping. Recently, two cases of boric acid precipitation due to PWSCC were reported on the bottom head surface of SG in Korea [5].

The PWSCC resistance of Ni base alloys with intergranular carbide morphologies is higher than those with intragranular ones in low oxygen primary water of PWR [6]. On the other hand, in acidic oxidized solutions like sodium sulfate or sodium tetrathionate solutions ($Na_2S_4O_6$), the Ni base alloys with a lot of carbides at the grain boundaries show less SCC resistance [7-9]. Thus grain boundary carbides or Cr depletion of the Ni base alloys behave differently on the SCC in each condition. The objective of the paper is to show a different role of the grain boundary carbides on the SCC in oxidized acidic solution and simulated PWR primary water and to review the increase of PWSCC resistance mechanism of Ni base alloys.

2. EXPERIMENTAL PROCEDURE

2.1 Material

High temperature mill-annealed (HTMA) Alloy 600 SG tubing was used for this investigation. The thickness and outside diameter of the specimen was 1.09 mm and 19.05 mm, respectively. The HTMA for as-received tubing was at 1060~1070 °C, which is a high enough temperature to ensure that most carbon in the alloy is dissolved and that no carbide precipitates remain. Table 1 shows information of the test material.

Table 1. Information of the Test Material Alloy 600 Tubing and Forged Alloy 600

(a) Alloy 600 HTMA tubing for room temperature SCC test													
Chemical compositions													
C	Mn	Si	P	S	Ni	Cr	Ti	AI	Co	Cu	Fe	N	B
0.025	0.21	0.19	0.005	<0.001	74.19	15.52	0.29	0.22	0.018	0.012	9.3	0.024	<0.0005

Maker: Inco/Valinox, Heat : NX8524, OD/thickness : 3/4"(19.05mm)/1.09mm, Thermal History: 1024 °C/3 minutes then cooled to 500 °C for 7 minutes, YS(@20): 241 MPa, UTS(@20): 662 MPa, EL(@20): 39.2%, Grain size: 5.5

(b) Forged Alloy 600 material for high temperature PWSCC test													
Chemical compositions													
C	Mn	Si	P	S	Ni	Cr	Ti	AI	Co	Cu	Fe	N	B
0.055	0.60	0.48	0.005	<0.001	75.80	15.45	0.18	0.17	0.06	0.03	6.98	-	-

Maker: Schmidt + Clemens Edelstahlwerk (Germany)
Dimension : 120 mm (Φ) x 130 mm (L), Processing : Hot formed, Heat treated, Machined
Heat Treatment : 950 °C, for 3 hrs, water cooled, 0.2% YS(@20): 241 MPa, UTS(@20): 552 MPa, EL(@20): 30 %
Related Spec. : ASTM B 564

For PWSCC test, forged Alloy 600 material was used. The original dimension of the material was 120 mm in diameter, 130 mm in length, respectively. The hot formed material was heat treated for 3 hours at 950 °C then water cooled.

2.2 SCC Test in Acidic Solution

The as-received tubing was heat treated at 600 °C for 48 hours in a vacuum to sensitize the material for easier cracking in the test solution ($Na_2S_4O_6$) at room temperature. The C-ring specimens were prepared according to the ASTM G38 [10]. They strained to a constant deflection in the range of plastic deformation using Alloy 600 bolts and nuts, as shown schematically in Fig. 1. The apex of the specimens was ground with # 1000 emery paper before the deflection. The relationship between elastic stress at the apex and the variation of tube diameter is described as follows [10].

$OD_f = OD - \Delta$ .... Eq.(1)

$\Delta = f\pi D^2/4EtZ$

where,

OD : Outside diameter before stressing
OD_f : Outside diameter of stressed C-ring
Δ : Change of OD giving desired stress
f : Applied stress
D : Mean diameter (OD-t)
t : Wall thickness
E : Modulus of elasticity
Z : Correction factor for curved beams

If one considers only the Hooke's law and Eq (1), it would not be possible to apply over 100% of yield stress on the C-ring apex. However, it is possible to load the C-ring sample until the elastic strain reaches at Ee as shown in Fig. 2.
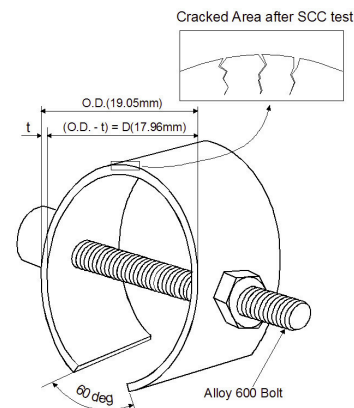

Fig. 1. Schematic of the C-ring Specimen for the Test.(C-ring Apex is Loaded and Unloaded by Stressing and un Stressing the Bolt and Nut)
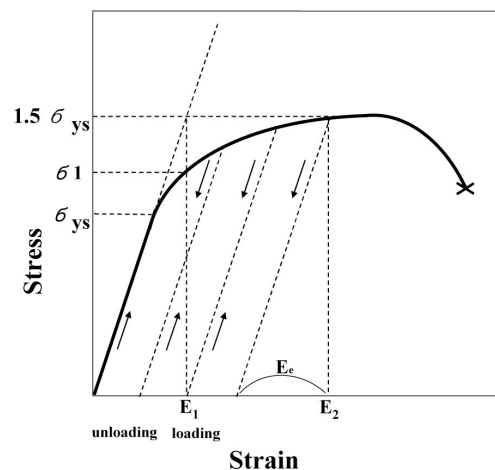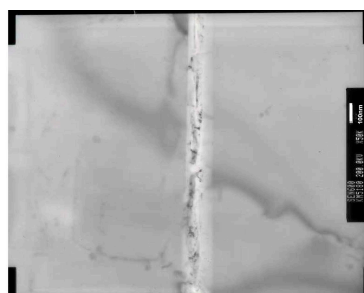

Fig. 2. Principle of a Loading and Unloading Method in C-ring Specimens Up to Load Over Yield Strength.

In these experiments, the stress was applied on the C-rings by repeating the process of loading, unloading, and reloading to increase an elastic portion of deformation at room temperature. It was then possible to apply a stress above 100% of yield stress according to the Eq. (1). The applied stress on the C-ring test specimens was 90%, 100%, 125%, and 150% of the room temperature yield stress of the material.

The stress loaded C-ring specimens were cleaned with acetone and distilled water. The specimens were then exposed to 0.01 M or 0.1 M of $Na_2S_4O_6$ test solution at room temperature for up to 72 hours. The apex of test specimens was examined with a low magnification stereo microscope during the exposure at 6 hour intervals to determine crack initiation time.

2.3 SCC Test in Simulated PWR Primary Solution

In the present PWSCC experiment, 1/2 compact tension (CT) specimens were used and its dimensions are shown in Figure 3.

Before the PWSCC test, the CT specimen was fatigue pre-cracked to a length of about 2 mm in air. The PWSCC test was conducted under the simulated primary water environmental conditions of 1200 ppm of B and 2 ppm of Li under internal pressure of 2300 psi(or 15.9 MPa) at 340 °C. Dissolved oxygen(DO) content and hydrogen partial pressure of the water was below 5 ppb and 14.3 psi (or 0.1 MPa), respectively. The maximum stress intensity factor at a crack tip was maintained at 30 MPa√ m. Major experimental parameters such as the temperature, load, displacement, pH, electric conductivity, ECP and DO were being monitored and collected by PC through an A/D converter. A direct current of 5 A was applied to the CT specimen, and the current was periodically reversed via a programmed current source. Voltage drops were measured from the CT specimen and a reference coupon through digital voltmeters. The crack length was then calculated using the Hicks and Pichard (H&P) equation on the basis of the measured voltages [11,12]. The reference coupon prepared with the same material as the CT specimen was equipped to calibrate the material's resistivity changes occurring after long term exposure at high test temperature. A schematic diagram of the test loop is shown in Figure 4.

3. RESULTS AND DISCUSSION

3.1 Carbide Precipitation and SCC Susceptibility

Figure 5 is of scanning electron micrographs (SEM) of the sensitized testing material. The average grain size is about 50 to 100 μm and the carbides are well grown up as shown in the micrographs. Figure 6 is of transmission electron micrographs (TEM) of the material showing clear formation of carbides and their morphology on the grain boundaries. It is evident that the samples are fully sensitized by the heat treatment.

Fig. 3. Dimensions of a 1/2 CT Specimen for PWSCC Test.

Fig. 4. Schematic Diagram of the PWSCC Test Loop.

(a)

(b)

Fig. 5. SEM Micrographs Showing Grain Boundary Carbides of Sensitized Alloy 600 Tube.
(a) SEM micrograph showing grain structure and grain boundary carbides
(b) Enlarged SEM micrograph showing grain boundary carbides

(a)

(b)

Fig. 6. TEM Micrographs Showing Grain Boundary Carbides in a Sensitized Alloy 600 Tube.
(a) TEM micrograph showing carbides along the grain boundary.
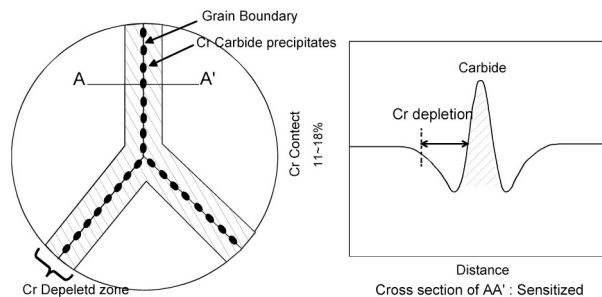(b) Enlarged carbides morphology of the sensitized alloy 600.

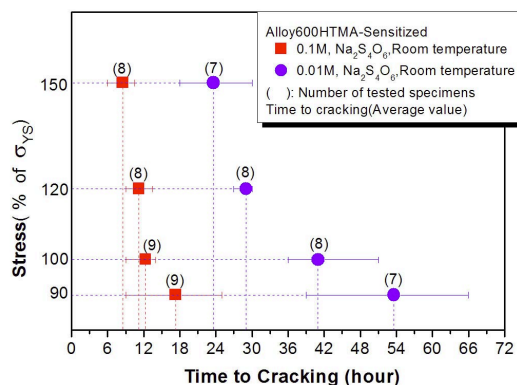Fig. 7. Schematic of Cr Depletion in Sensitized 304 Stainless Steel.

Fig. 8. Effect of Applied Stress on Time to Cracking of Sensitized Alloy 600 in Acidic Solution at Room Temperature.
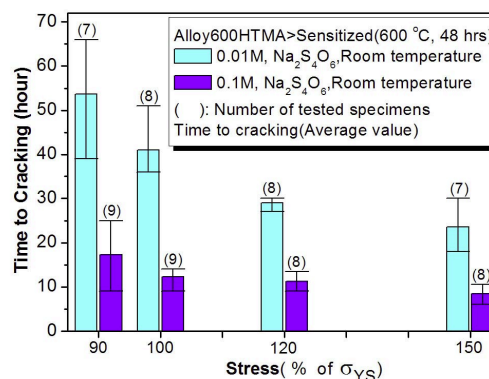

Fig. 9. IGSCC Susceptibility Versus Applied Stress on Sensitized Alloy 600 in Acidic Solution at Room Temperature.

Sensitization of stainless steel (SS) is caused by the precipitation of chromium carbides along the grain boundaries. This precipitation depletes the Cr content near the grain boundaries, thereby decreasing its corrosion resistance. The Cr depletion near grain boundaries of sensitized Type 304 SS is schematically shown in Figure 7. In the case of austenitic stainless, chromium carbides and a chromium depleted zone form at a maximum rate of around 815 °C, and the rate decreases slowly at lower temperatures down to 482 °C. The sensitization rate is a complex function of a number of factors. For austenitic stainless steels, the sensitization is prevented by keeping the carbon content of the alloy below 0.03% e.g., Type 304L, 316L. In ferric stainless steels, the formation of chromium depleted zone is only suppressed by combining all carbon and nitrogen in the alloy with titanium or niobium.

The austenitic stainless steels can be quenched above 871 °C to prevent precipitation, but ferritic stainless steels cannot be quenched rapidly enough.

In the mid-seventies, intergranular stress corrosion cracking (IGSCC) problems occurred in the heat-affected zones of Type 304 stainless steel welded piping which were used in BWRs. One of the main causes of SCC was the presence of chromium carbide precipitates and chromium depletion at the grain boundaries of the austenitic stainless steel, i.e., sensitization.

Ni base alloys also show chromium depletion along the grain boundaries when they are exposed to certain high temperatures and slowly cooled to room temperature, depending on the carbon content of the materials. These sensitized Ni base alloys exhibit high intergranular corrosion rates in oxidized acidic solutions at room or high temperatures (for example, $Na_2S_4O_6$ solutions)[7].

Figures 8 and 9 show the results of our C-ring tests for the sensitized HTMA Alloy 600 in 0.1 and 0.01M $Na_2S_4O_6$ solutions at room temperature. Cracking susceptibility is plotted in terms of the applied stress and time of cracking. A cracking time as short as 7 hours was observed for the specimen loaded at 150% of the yield stress. The cracking
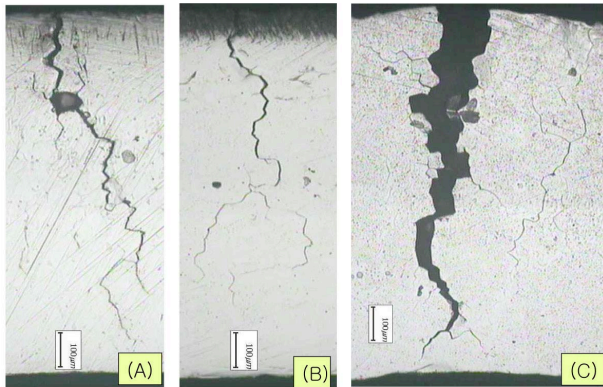
Fig. 10. Optical Micrograph Showing Cross Section of Crack in C-ring Specimen in a Sensitized Alloy 600 with 90~120% Yield Stress Tested in 0.1 M $Na_2S_4O_6$ solution at RT, (A) 90%, (B) 100%, (C) 120% Yield Stress.

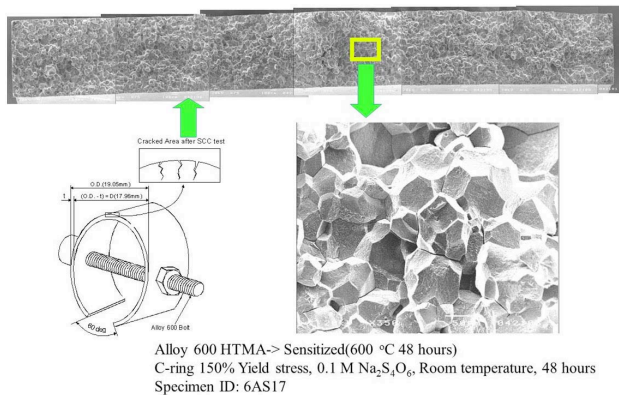Alloy 600 HTMA-> Sensitized(600 °C 48 hours)
C-ring 150% Yield stress, 0.1 M $Na_2S_4O_6$, Room temperature, 48 hours
Specimen ID: 6AS17

Fig. 11. Typical Fracture Surface of IGSCC of Sensitized Alloy 600.

Fig. 12. Crack Growth Rate of Two Alloy 600 Having Different Microstructures (Skyblue Circle: Intragranular Carbides, Red Circle:well Developed Intergranular Carbides). *Note: Skyblue Circle, Red Circles are Obtained in this Study.*

Fig. 13. PWSCC Susceptibility vs. Grain Boundary Carbide Coverage[4].

time here means time to observe a crack first on the specimen apex by a low magnification microscope at every 6 hour interval to determine crack initiation time. Figure 10 shows a cross section of cracked C-ring specimens tested in 0.1 M sodium tetrathionate solution. The typical cracking mode of the sensitized Alloy 600 is intergranular as shown in Figure 11. These results clearly show that the sensitized microstructure of Alloy 600 is very susceptible to SCC in the oxidized acidic solution, which is a similar behavior to the cracking of sensitized SS.

Some researchers pointed out that grain boundary carbide and chromium depletion areas

formed in the sensitized alloy 600 accelerate the SCC initiation and propagate under the acidic condition. One of the explanations considered is that enriched nickel in the chromium depletion zone is easy to dissolve in an acidic solution[13]. So, the corrosion resistance of grain boundary with chromium depletion zone is low in the acidic solution.

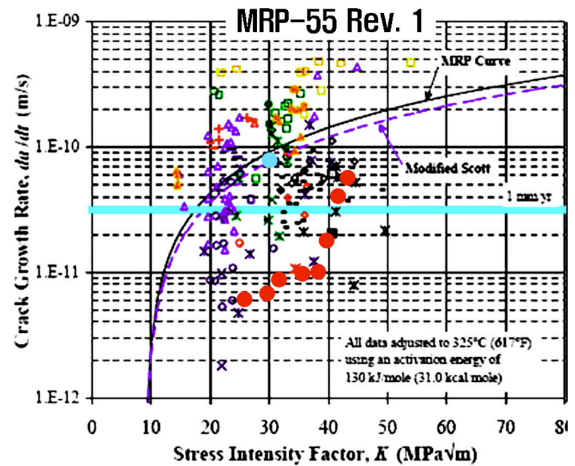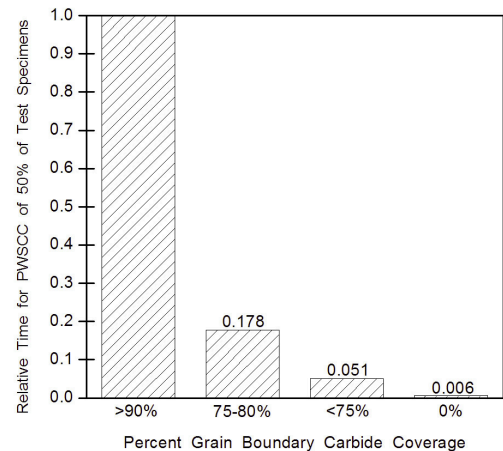PWSCC resistance of the two Alloy 600 obtained in this work is plotted in Figure 12. It is believed that the main

reason for the different crack growth rate (CGR) of the two alloys is from micro structural differences, especially from the differences in the grain boundary carbide morphologies of the materials.

Thermal treatments which produce chromium carbide at grain boundaries provide better resistance to SCC in high purity water, as reported by Coriou in 1973 [14]. It is generally considered that Alloy 600 with many carbides on the grain boundary were found to be more resistant to PWSCC, whereas those with many intragranular carbides are the most susceptible [15-17].

Figure 13 illustrates the susceptibility to the PWSCC of Ni base alloys in primary water, in terms of grain boundary carbide coverage[3]. The best resistance to the PWSCC of Alloy 600 in primary water appears to be associated with the chromium carbide decorated microstructure at the grain boundaries.

3.2 Fabrication Variables and SCC Susceptibility

The main fabrication variables which control the carbide morphology in Alloy 600 are the final forming process and annealing conditions. These factors significantly affect PWSCC susceptibility of the materials [4].

Presence of Cr carbides within grains and at grain boundaries is influenced by the prior and the final forming, heating and annealing processes. The material is cold worked during final forming operations and then recrystallized during the final annealing treatment with cooling resulting in new grain boundaries. The solubility of the carbides during annealing is a strong function of the annealing temperature. At a low annealing temperature, carbides do not fully go into the base alloy so large amounts of carbides remain within the former grains after cooling and there are few grain boundary carbides. For example, carbides in a material with 0.04 % of carbon content can be fully solutionized at 1030 °C based on the carbon solubility as seen in Fig. 14[18].

Figure 15 shows different microstructures depending on the fabrication history of Ni base alloys[19]. The material with a final annealing at high temperature shows intergranular carbides, whereas the one with a final annealing at a low temperature shows intragranular carbides.

At a high annealing temperature, carbides dissolve almost completely into the solution and the grains grow in size which reduces the grain boundary surface area, and carbides precipitate at the new grain boundaries when it cools down. Therefore, a high temperature annealing results in large grains, copious grain boundary (intergranular) carbides, and few intragranular carbides.

3.3 Beneficial Effect of Intergranular Carbides on PWSCC Resistance

The occurrence of PWSCC of Alloy 600 strongly depends on the presence of intergranular carbides. Intergranular carbides are formed by mill-annealing at high temperatures (e.g., 1065 °C) during the final 15 hour heat and thermal treatment at 705 °C . This heat treatment makes Alloy 600 tubes resistant to PWSCC. On the other hand, low mill-annealing temperatures produce intragranular carbides, which make tubes susceptible to PWSCC.

Bruemmer proposed a model to explain the role of intergranular carbides [6]. Grain boundary carbides promoted crack blunting due to their effectiveness as dislocation sources, as illustrated in Fig. 16. Hwang et. al. also have showed different dislocation behaviors from grain boundary with and without grain boundary carbide structures[20, 21]. As reported by Bruemmer [6], the larger the dislocations in alloy, the greater the number of carbides at the grain boundaries, the more dislocation sources will be present to blunt the crack. Smialowska and Rebak proposed another possible explanation that Alloy 600 material passivates more readily under the presence of grain boundary carbides [22, 23].
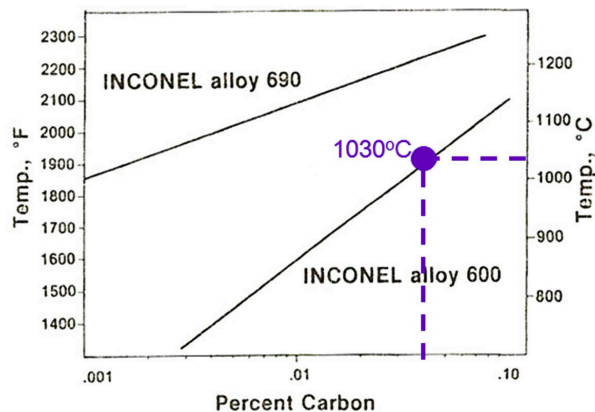

Fig. 14. Annealing Temperature and Carbon Contents in Alloy 600 and 690[18].
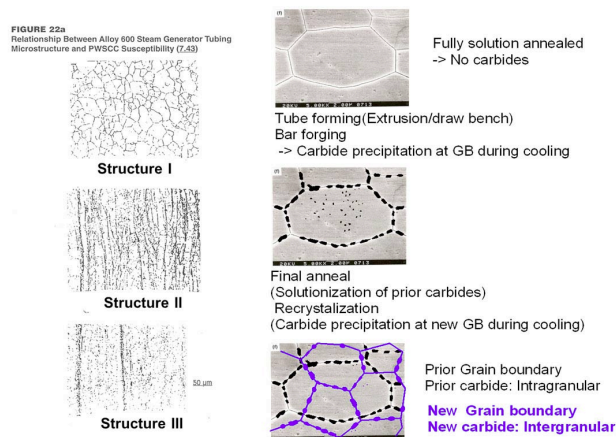

Fig. 15. Different Microstructure Depending on Fabrication History of Ni Base Alloys[19].
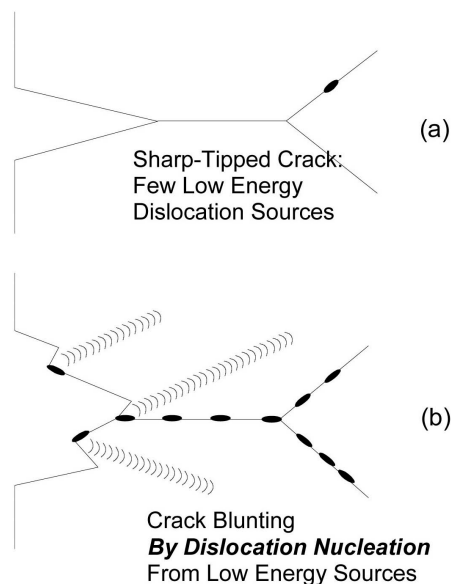

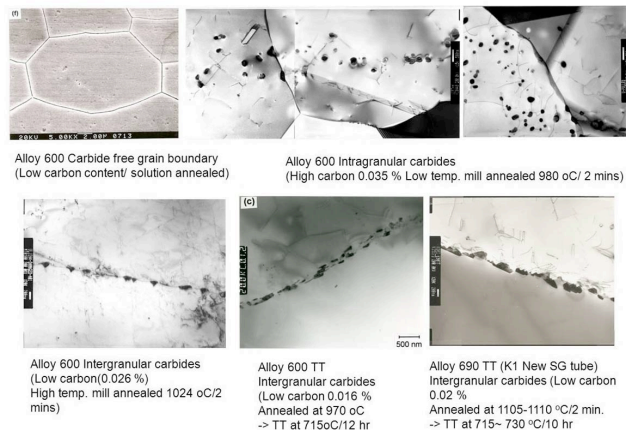Fig. 16. Beneficial Effect of Intergranular Carbides on PWSCC of Ni Base Alloys [6].

Fig. 17. Different Carbide Precipitation in Ni Base Alloys Depending on Carbon Contents or Thermal History.

Undissolved carbon in materials with high carbon content hinders grain growth during heat treatments, so a small grain sized microstructure is developed. The small grain alloys shows high yield strength which results in a susceptible microstructure. Likewise, low temperature annealing causes an intragranular carbide structure which is susceptible to PWSCC.

Figure 17 shows a comparison of different microstructures which have a different carbon content or a different thermal history. The typical examples of the different microstructures shown in Fig. 17 are categorized as below:

- Less grain boundary carbides due to a low carbon content or solution annealing.
- Intragranular carbides with high carbon, e.g., a low temperature mill annealed structure at 980 °C for 2 minutes of 0.035 % of carbon. (LTMA Alloy 600)
- Intergranular carbides with low carbon (0.026 %), a high temperature mill-annealing at 1024 °C for 2 minutes.(HTMA alloy 600)
- Intergranular carbides with low carbon (0.016 %), annealed at 970 °C, then thermally treated at 715 °C for 12 hours (Thermally treated Alloy 600)
- Intergranular carbides with low carbon (0.02 %), annealed at 1105-1110 °C for 2 minutes, then thermally treated at 715~ 730 °C for 10 hours. (Thermally treated Alloy 690).

4. CONCLUSIONS

The role of grain boundary carbides in the SCC behavior of Ni base alloys was investigated.

(a) Sensitized Ni base alloys exhibit a high intergranular corrosion rate in oxidized acidic solution. The sensitized Alloy 600 showed a similar SCC behavior of sensitized SS in the oxidized acidic solution.

(b) PWSCC resistance of Alloy 600 in primary water

environment appears to be associated with the Cr carbide decorated microstructure at grain boundaries.

(c) Grain boundary carbides promote crack blunting due to their effectiveness as a dislocation source. The greater the number of carbides at the grain boundaries, the more dislocation sources are present to blunt the crack.

ACKNOWLEDGEMENT

REFERENCES

[1] IAEA Technical Document No. NP-T-3.13, *Stress Corrosion Cracking in Light Water Reactors: Good Practices and Lessons Learned*, p. 1, Vienna, Austria IAEA (2011).
[2] Materials Reliability Program : *PWSCC of Alloy 600 Type Materials in Non-Steam Generator Tubing Applications — Survey Report through June 2002: Part 1: PWSCC in Components Other Than CRDM/CEDM Penetrations* (MRP-87), EPRI, Palo Alto, CA, 1007832, (2003)
[3] NUREG 1823, *U.S. Plant Experience With Alloy 600 Cracking and Boric Acid Corrosion of Light-Water Reactor Pressure Vessel Materials*, U.S. Nuclear Regulatory Commission, Office of Nuclear Regulatory Research Washington, DC 20555-0001, (2005)
[4] EPRI TR-103696, *PWSCC of Alloy 600 Materials in PWR Primary System Penetrations*, EPRI, Palo Alto, California, USA, (1994).
[5] S.S. Hwang, et. al., *Failure Analysis on Steam Generator Drain Nozzle in Yonggwang Unit 4-Final Report*, KAERI/CR-329/2009, (2009).
[6] S. M. Bruemmer, *Corrosion*, vol. 44, p.782 (1988).
[7] M.C.Tsai, et.al., *Corrosion science*, vol. 34, p.741 (1993).
[8] W.T. Tsai, et.al., *Corrosion*, vol. 50, p.98 (1994).
[9] W.T. Tsai, M.J.Sheu and J.T.Lee, *Corrosion Science*, vol. 38, p.33 (1996).
[10] ASTM G38, '*Standard Practice for Making and Using C-ring Stress-Corrosion Test Specimens*', (1984).
[11] E647-00, Standard Test Method for Measurement of Fatigue Crack Growth Rates, ASTM International, PO Box C700, West Conshohocken, PA 19428, (2000)
[12] M. A. Hicks and A. C. Pickard, A Comparison of Theoretical and Experimental Methods of Calibrating the Electrical Potential Drop Technique for Crack Length Determination, Int. J. of Fracture, vol. 20, p. 91, (1982)
[13] Hirotaka Kawamura et. al., *Corrosion Engineering*, vol. 48, p.99-111 (1999)
[14] H.Coriou, et. al. 'Historical Review of the Principal Research Concerning the Phenomena of Cracking of Nickel Base Austenitic Alloys.' *Proceedings of Conference on Fundamental Aspects of Stress Corrosion Cracking and Hydrogen Embrittlement of Iron Base Alloys*. Unieux-Firminy France, June 12-16, 1973, NACE-5.
[15] EPRI NP-3051, *Optimization of metallurgical variables to improve corrosion resistance of Inconel alloy 600*, EPRI, Palo Alto, California, USA (1983).
[16] EPRI NP-5987-SP, *PWSCC behavior of thermally treated alloy 600*, EPRI, Palo Alto, California, USA (1988).

[17] Garriga Majo, D., et al. *Prediction of the In-service behavior of alloy 600 tubes used in steam generators of pressurized water reactors*, Colloque international, Fontevraud II, SFEN, Sept. 10-14, (1990).

[18] J.M.Sarver, J.R. Crum, W.L. Mankins, *Corrosion*, vol. 44, p. 288 (1989).

[19] EPRI TR-103824, 'Steam Generator Reference Book', p.7-40, EPRI, Palo Alto, California, USA (1994).

[20] S.S.Hwang, *Jr. of Nuclear Materials*, vol. 275, p.28 (1999)

[21] S.S.Hwang, *Corrosion Science and Technology*, vol. 7, p.189 (2008)

[22] Z.Szkalska-Smialowska, Factors influencing IGSCC of alloy 600 in primary and secondary waters of PWR steam generators, 4th Symposium on environmental degradation of materials in nuclear power systems-Water Reactors, p.6-1Jekyll Island, Georgia, August 6-10, 1989, NACE, Houston, TX, (1990).

[23] R.B.Rebak, and Z.Szkalska-Smialowska, The mechanism of stress corrosion cracking of alloy 600 in high temperature water, *Corrosion Science*, vol.38, pp.971-988, (1996).